Transient-State Kinetics of the Reaction of Aspartate Aminotransferase with Aspartate at Low pH Reveals Dual Routes in the Enzyme−Substrate Association Process†

Hideyuki Hayashi and Hiroyuki Kagamiyama*

Department of Biochemistry, Osaka Medical College, 2-7 Daigakumachi, Takatsuki 569, Japan

Received July 8, 1997⊗

ABSTRACT: In aspartate aminotransferase, the coenzyme pyridoxal 5′-phosphate forms a Schiff base with the ϵ-amino group of Lys258. The pH dependency of the steady-state kinetics of the overall reaction had indirectly suggested that the Schiff-base-unprotonated form of the enzyme (E_L) is the active species that binds the monoanionic form of aspartate (SH^+), the predominant species of the substrate in solution. In order to obtain direct information on the association process, we carried out transient-phase kinetics of the first half-reaction of the enzyme with aspartate at various pH. The disappearance of E_L (λ_{max} = 358 nm) was fast and independent of pH, but the disappearance of E_LH^+ (Schiff-base-protonated form, λ_{max} = 430 nm) was slow and dependent on pH. At pH values below 6.8 and low concentrations of aspartate, the results could be interpreted to indicate that E_L reacts rapidly with SH^+ to form the pyridoxamine 5′-phosphate form of the enzyme (E_M), and the reaction of E_LH^+ proceeds via the route $E_LH^+ \rightleftarrows E_L \rightleftarrows E_M$, where the first step was found to be rate limiting from the pH jump/drop study of the enzyme. At higher pH values, the rate of disappearance of E_LH^+ became larger than expected from the above scheme. This deviation became apparent with increasing pH, and could be excellently explained if we consider that it is due to the reaction of E_LH^+ with the dianionic form of aspartate (S). Thus, the formation of the Michaelis complex of aspartate aminotransferase and aspartate can proceed via two routes; route A is the association of E_L with SH^+ to form $E_L{\cdot}SH^+$, which converts intramolecularly to $E_LH^+{\cdot}S$, and route B is the association of E_LH^+ with S to form $E_LH^+{\cdot}S$ directly. $E_LH^+{\cdot}S$ is the prerequisite structure for further processing of the substrate by the enzyme. The reactions of E_M and oxo acids yielded almost exclusively E_L and SH^+, and therefore route B does not seem to play an essential role in the overall reactions of the enzyme. Route B, however, may be important in the reaction mechanisms of other pyridoxal 5′-phosphate enzymes which have only the E_LH^+ form.

Aspartate aminotransferase (aspartate: 2-oxoglutarate aminotransferase, EC 2.6.1.1; AspAT)[1] is a pyridoxal 5′-phosphate (PLP)-dependent enzyme and catalyzes the reversible transfer of the amino group of aspartate to 2-oxoglutarate by the following ping-pong Bi Bi mechanism:

$$\text{aspartate} + E_L \rightleftarrows \text{oxalacetate} + E_M \quad (1)$$

$$\text{2-oxoglutarate} + E_M \rightleftarrows \text{glutamate} + E_L \quad (2)$$

Here E_L and E_M denote the PLP form and the pyridoxamine 5′-phosphate (PMP) form of the enzyme, respectively. The three-dimensional structures have been solved both for the cytosolic and mitochondrial isoenzymes (*1*−*4*) as well as for the *Escherichia coli* enzyme (*5*, *6*). Two active sites are formed symmetrically near the subunit interface of the dimeric enzyme, and in each active site PLP forms a Schiff base with the ϵ-amino group of Lys258.[2] The Schiff base undergoes reversible protonation/deprotonation with an apparent pK_a near 6.5 (*8*, *9*). The pH dependence of the kinetic parameters of the overall reaction of AspAT (eq 1 plus eq 2) has been extensively studied (*10*). The most outstanding feature of the kinetic results was that the k_{cat}/K_m value for aspartate decreases at low pH with a slope of 1 and gives a pK_a value around 6.5, corresponding to the pK_a of the Schiff base. From this, an accepted mechanism has been proposed for the catalytic action of AspAT (*11*−*13*, described as a part of Scheme 1). According to the mechanism, the enzyme form with unprotonated Schiff base (E_L) is the active species and accepts the monoanionic form[3] of the substrate aspartate (SH^+) to yield the first Michaelis complex ($E_L{\cdot}SH^+$ in Scheme 1). The proton on the ammonium group of aspartate then moves to the imine nitrogen of the PLP−Lys258 Schiff base to form the second Michaelis complex ($E_LH^+{\cdot}S$ in Scheme 1). The latter complex easily undergoes transaldimination, resulting in the formation of the PLP−aspartate Schiff base and the free ϵ-amino group of Lys258 (E_3 in

† This work was supported by Grants-in Aid (06680628 to H.H. and 14454160 to H.K.) from the Ministry of Education, Science, Sports, and Culture of Japan, and by a Research Grant from the Japan Society for the Promotion of Science (RFTF96L00506).

* Author to whom correspondence should be addressed.

⊗ Abstract published in *Advance ACS Abstracts,* October 15, 1997.

[1] Abbreviations: AspAT, aspartate aminotransferase (aspartate: 2-oxoglutarate aminotransferase, EC 2.6.1.1); HEPES, 4-(2-hydroxyethyl)-1-piperadineethanesulfonic acid; MES, 4-morpholineethanesulfonic acid; TAPS, 3-(tris(hydroxymethyl)methylamino)propanesulfonic acid; MH buffer, buffer containing 25 mM MES-NaOH, 25 mM HEPES-NaOH, and 0.1 M KCl; HT buffer, buffer containing 25 mM HEPES-NaOH, 25 mM TAPS-NaOH, and 0.1 M KCl; PLP, pyridoxal 5′-phosphate; PMP, pyridoxamine 5′-phosphate; OA, oxalacetate.

[2] The amino acid residues are numbered according to the sequence of pig cytosolic aspartate aminotransferase (*7*).

[3] The two carboxylate groups are dissociated, and the amino group is protonated.

S0006-2960(97)01638-3 CCC: $14.00

Scheme 1: Mechanism of the Reaction of AspAT with Aspartate[a]

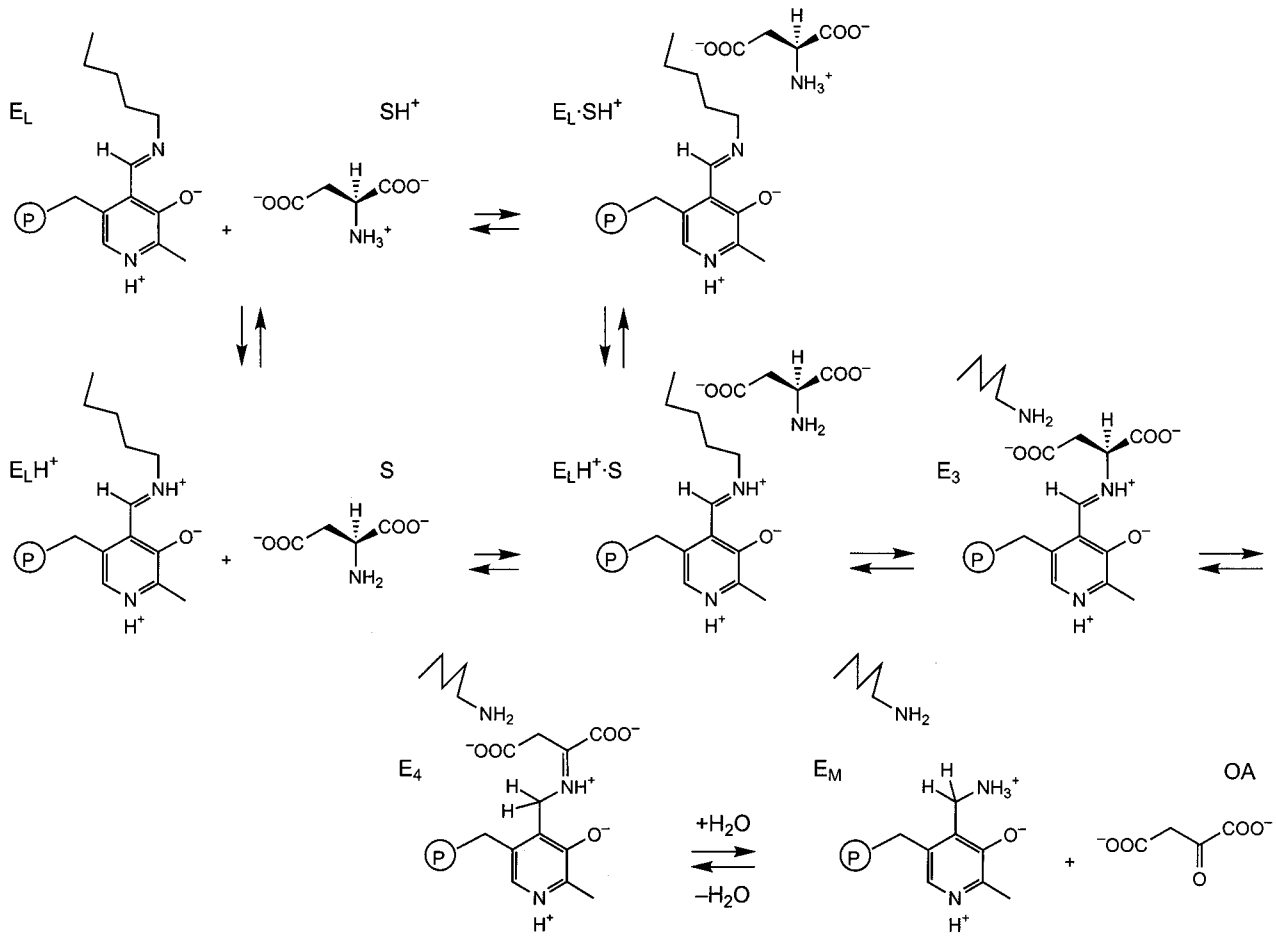

[a] The earlier proposals (*12*, *13*) did not take into account the association of E_LH^+ and S.

Scheme 1). The free ϵ-amino group then catalyzes the 1,3-prototropic shift of the PLP−aspartate Schiff base to the PMP−oxalacetate Schiff base (E_4 in Scheme 1), which decomposes to form E_M and oxalacetate.

In spite of this apparently straightforward explanation, a gap still exists between the kinetics and the catalytic mechanism of AspAT. The kinetic parameters discussed above are those for the overall reaction ($k_{cat}^{overall}$ and $K_m^{overall}$, see ref 14 for definition) and are indirectly related to the reaction mechanism. Theoretical considerations showed that $k_{cat}^{overall}/K_m^{overall}$ is equal to $k_{cat}^{half}/K_m^{half}$, which is the k_{cat}/K_m value for the half-reaction and is directly related to the association of the enzyme and the substrate (*14*, *15*). Thus, the preceding discussions on the reaction mechanism of AspAT have been based on the assumption that $k_{cat}^{overall}/K_m^{overall}$ can be used as a substitute for $k_{cat}^{half}/K_m^{half}$. Although this is a reasonable assumption, acid−base chemistry of the half-reaction itself is required in order to pursue further the reaction mechanism of AspAT, because it would give more direct information on the catalytic mechanism of AspAT. In this study, we first attempted to determine the pH dependence of the k_{cat}^{half} and K_m^{half} values, by carrying out the transient-state kinetics of the reaction of AspAT with aspartate at various pH values. The results showed, however, complex kinetic behavior at low pH. Analysis of the reactions, together with pH jump/drop studies, revealed that the anomalous kinetics at low pH was due to the slow interconversion between the Schiff-base-protonated species (E_LH^+) and the unprotonated species (E_L) of the enzyme. Additionally, we could separate kinetically the two possible routes for association of the enzyme and the substrate, the one begins with $E_L + SH^+$ and the other with $E_LH^+ + S$; the two mechanisms cannot be distinguished by the steady-state kinetics of the overall reaction due to the "principle of kinetic equivalence" (*16*, *17*). The significance of the two routes in the half and the overall reactions of AspAT and in the reaction mechanisms of other PLP enzymes is discussed.

EXPERIMENTAL PROCEDURES

Chemicals. E. coli AspAT was obtained by the method described previously (*9*) using *E. coli* JM103 containing pUC19-*aspC*. PMP was obtained from Sigma (St. Louis, MO). All other chemicals were of the highest grade commercially available.

Spectroscopic Analysis. Absorption spectra were measured using a Hitachi (Tokyo, Japan) U-3300 spectrophotometer at 298 K. The buffer solution contained 50 mM buffer component(s) and 0.1 M KCl. The buffer components used were MES-NaOH, HEPES-NaOH, and TAPS-NaOH. Protein concentrations were generally $(1-3) \times 10^{-5}$ M in subunits. The concentration of the AspAT subunit in solution was determined spectrophotometrically. The apparent molar extinction coefficients used were $\epsilon_{app} = 4.7 \times 10^4$ M^{-1} cm^{-1} for the PLP form of the enzyme and $\epsilon_{app} = 4.6 \times 10^4$ M^{-1} cm^{-1} for the PMP form of the enzyme at 280 nm (*18*).

Kinetic Analysis. Stopped-flow spectrophotometry was performed using an Applied Photophysics (Leatherhead, U.K.) SX.17MV spectrophotometer at 298 K. The exponential absorption changes were analyzed with the program provided with the apparatus. The dead time was 2.3 ms

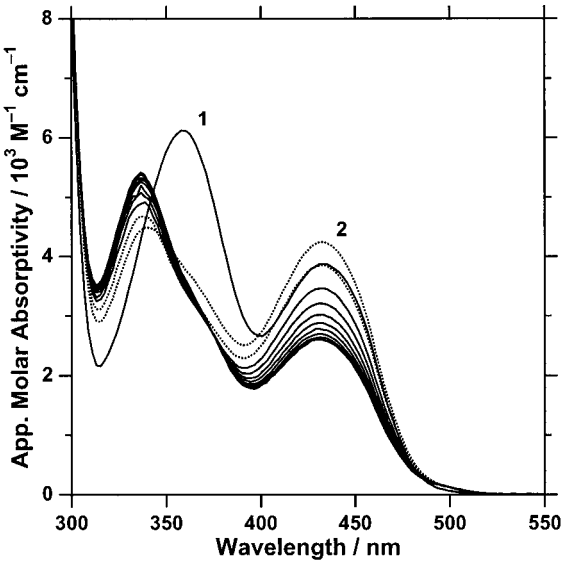

FIGURE 1: Time-dependent absorption change of AspAT on reaction with aspartate at pH 7.0, 298 K. AspAT (28 μM, Curve 1) was reacted with 2 mM aspartate in MH buffer, pH 7.0, in an Applied Photophysics SX.17MV stopped-flow spectrophotometer equipped with a photodiode array detector. Absorption values were collected at 2.2 nm intervals between 300 and 550 nm, at $t = 2.3$, 3.64, 6.2, 8.76, 11.32, 13.88, 16.44, 19.0, 21.56, and 24.12 ms. The spectrum for $t = 2.3$ ms (Curve 2) and that for $t = 3.64$ ms are drawn in dotted lines in order to be distinguished from the rest of the spectra. After $t = 6.2$ ms, the absorption band at 430 nm gradually decreased with a concomitant increase in the 330-nm absorption, and these time-resolved spectra showed an isosbestic point at 377 nm. Therefore, the fast phase reaction was monitored at 377 nm in order to minimize the perturbation due to the slow phase.

under a pressure of 500 kPa as determined from the reaction of 2,6-dichlorophenolindophenol and ascorbic acid (*19*). The apparent rate constants obtained were then analyzed for their dependency on the substrate concentration by nonlinear regression with the software Igor Pro (Ver. 3.03, WaveMetrics, Lake Oswego, OR). Multiple-wavelength stopped-flow analysis was carried out on an SX.17MV instrument equipped with a photodiode-array detector. The spectra were taken at $t = 1.08$ ms, 3.64 ms, and then at intervals of 2.56 ms, where t is the time elapsed after the "true" mixing (corrected for the dead time). However, because the spectrum at $t = 1.08$ ms is taken during the flow, this should be considered to represent the spectra at $t = 2.3$ ms.

RESULTS

Spectral Change of AspAT on Reaction with Aspartate at Low pH. At pH 8.0, the PLP−Lys258 Schiff base exists almost as an unprotonated form absorbing at 358 nm (E_L in Scheme 1). The spectral change of AspAT on reaction with aspartate proceeded in a single exponential manner (*18*). The apparent rate constant for the exponential change was analyzed for its dependence on aspartate concentration, and the kinetic parameters for the "half"-reactions of the PLP form of AspAT and amino acids and the PMP form with oxo acids were obtained. These parameters could excellently explain the kinetic parameters for the overall reactions (*18*). We extended the analysis to lower pH values. Figure 1 shows the spectral change of the reaction of AspAT with 2 mM aspartate at pH 7.0. At this pH, AspAT has two absorption bands at 430 and 358 nm (Curve 1), corresponding to the Schiff-base-protonated form (E_LH^+ in Scheme 1) and the unprotonated form (E_L in Scheme 1), respectively (*8*, *20*). On reaction with 2 mM aspartate, the absorption band at 358 nm rapidly decreased. At $t = 6.2$ ms, where the change in absorption around 350−380 nm due to the disappearance of the 358-nm band is almost over, significant absorption remained at 430 nm and gradually decreased over a time scale of about 20 ms. This indicates that E_L reacts rapidly with the substrate, but E_LH^+ more slowly. Single-wavelength stopped-flow spectroscopic analysis showed that the absorbance changes both at 430 and 377 nm proceeded

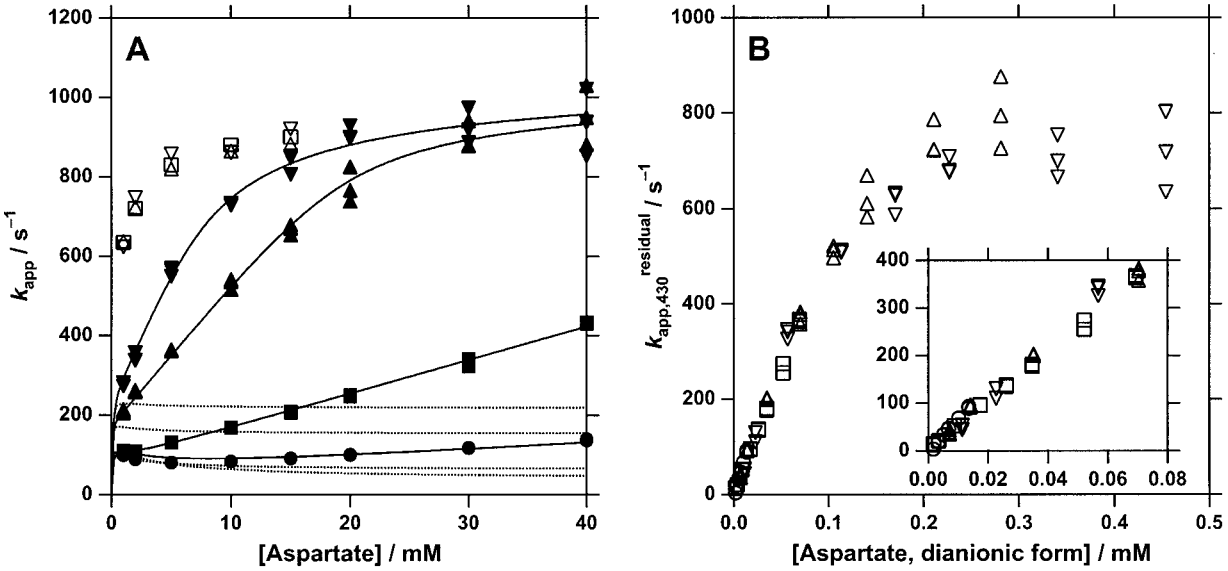

FIGURE 2: Dependence of the apparent rate constant for the absorption change on aspartate concentration at various pH values. AspAT (28 μM) was reacted in MH buffer with various concentrations of aspartate at 298 K, and the absorption change was monitored either at 430 nm and at 377 nm. (A) The apparent rate constant (k_{app}) was obtained from the exponential absorption change and was plotted against the aspartate concentration. Circles, pH 6.1; squares, pH 6.8; triangles, pH 7.4; reversed triangles, pH 7.7. Plots of $k_{app,377}$ and $k_{app,430}$ are indicated by open and filled symbols, respectively. The $k_{app,377}$ values could not obtained at pH 6.1 due to the weak absorption band at 358 nm. Dashed lines (pH 6.1, 6.8, 7.4, and 7.7 from bottom to top) are drawn according to eq 13 using the previously determined kinetic parameters (*18*). Solid lines are drawn according to eq 16 with $k_{+1}' = 5.4 \times 10^6$ M^{-1} s^{-1}. (B) Plots of $k_{app,430}^{residual}$ against the concentration of the dianionic form of aspartate (S). The inset shows the expansion of the points for low concentrations of S.

monoexponentially (data not shown; for the reason behind using 377 nm to monitor the disappearance of E_L, see the legend of Figure 1). The apparent rate constants, denoted as $k_{app,430}$ and $k_{app,377}$, respectively, were obtained for these spectral changes and were plotted against the concentration of aspartate (Figure 2A). The plots of $k_{app,377}$ showed a hyperbolic pattern identical to that observed at pH 8.0 (*9*, *18*). On the other hand, $k_{app,430}$ was always smaller than $k_{app,377}$ at any aspartate concentrations, and the plots of $k_{app,430}$ against the aspartate concentration did not fit a hyperbola at pH values below 7.4 (Figure 2A). This anomalous behavior of $k_{app,430}$ was most clearly seen at pH 6.1. At this pH, $k_{app,430}$ showed a decrease with increasing concentration of aspartate up to 5 mM (Figure 2A).

According to the accepted mechanism of AspAT, E_L is the active species that accepts the amino acid substrate, and E_LH^+ must be converted to E_L before reacting with the substrate (*13*). Assuming that the interconversion of E_LH^+ and E_L is rapid, the two forms disappear at the same rate. Apparently, this was not the case in the reaction of AspAT with aspartate (Figure 2A). In addition, the $k_{app,377}$ value was independent of pH (Figure 2A), indicating that there is essentially no flow from E_LH^+ to E_L that attenuates the net disappearance rate of E_L. We therefore examined the rate of interconversion of E_LH^+ and E_L using pH jump/drop spectrophotometric analysis.

AspAT Undergoes Slow Spectral Changes upon pH Jump/Drop. AspAT in MH buffer, pH 6.9, was quickly mixed with HT buffer, pH 9.6, or with MH buffer, pH 5.3, to yield a solution of pH 8.0 or 5.7, respectively, and the change in the absorption spectrum was followed in a stopped-flow spectrophotometer (Figure 3). That the pH of the solution changed rapidly within the dead time (2.3 ms) was confirmed using a pH indicator bromothymol blue (data not shown). The absorption changed in a single exponential manner at all wavelength values studied between 300 and 550 nm (~2.2 nm intervals). Thus, the interconversion of E_LH^+ and E_L was kinetically observable. The absorption spectra just after the pH jump (from 6.9 to 8.0) and pH drop (from 6.9 to 5.7) were estimated by extrapolating the time-resolved spectra during the exponential change to $t = 0$. These spectra were essentially superimposable with the initial spectrum (Figure 3). This indicates that the pH of the solution was changed rapidly without altering the protonation state of the Schiff base of AspAT, and then the Schiff base slowly exchanged a proton with the solvent to reach equilibrium. The apparent rate constant (k_{app}) for the exponential spectral change was found to be dependent on the final pH value and was independent of the pH of the initial enzyme solution (Figure 4). Therefore, the results of the pH jump/drop experiment were analyzed based on the following mechanism in which the rate of conversion from E_L to E_LH^+ and that from E_LH^+ to E_L are the function of the final pH value of the solution. In the mechanism, we assumed that $H_3{}^+O$ and OH^- undergo reversible binding to the enzyme before exchanging a proton with the Schiff base:[4]

$$E_L + H_3{}^+O \overset{K_1}{\rightleftharpoons} E_L{\cdot}H_3{}^+O \overset{k_1}{\underset{k_2}{\rightleftharpoons}} E_LH^+ + H_2O \qquad (3)$$

$$E_L + H_2O \overset{k_3}{\underset{k_4}{\rightleftharpoons}} E_LH^+{\cdot}OH^- \overset{K_4}{\rightleftharpoons} E_LH^+ + OH^- \qquad (4)$$

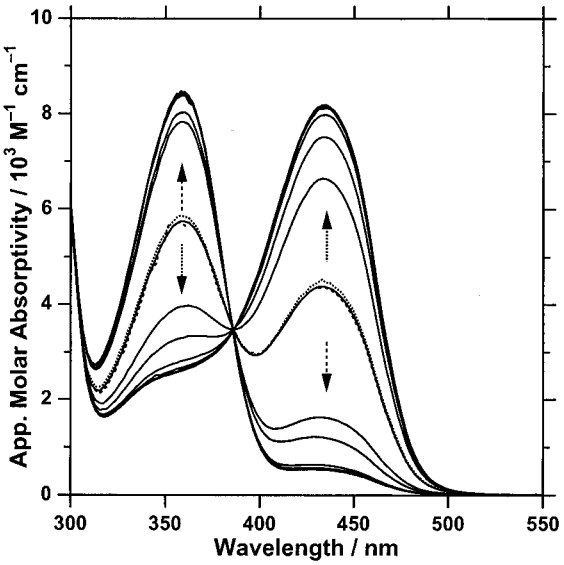

FIGURE 3: Changes in absorption spectrum of AspAT on pH jump/drop at 298 K. AspAT [25 μM in MH buffer (pH 6.9)] was mixed either with HT buffer (pH 9.6) or with MH buffer (pH 5.3) to give a final solution of pH 8.0 or pH 5.7, respectively. Spectra were taken in an Applied Photophysics SX.17MV stopped-flow spectrophotometer equipped with a photodiode array detector covering a wavelength range between 197 and 733 nm with 256 points. The solid line running between the arrows shows the spectrum before pH jump/drop (pH 6.9). The directions of the spectral changes are shown by dashed arrows (pH jump from 6.9 to 8.0) and dotted arrows (pH drop from 6.9 to 5.3). The spectral transitions were shown by sets of spectra at $t = 2.3$, 3.64, 6.2, 8.76, 11.32, 13.88, 16.44, 19.0, 21.56, and 24.12 ms. Extrapolation of these time-resolved spectra to $t = 0$ yields the spectra just after changing the pH of the solution, and these are shown by the dashed (pH jump) and dotted (pH drop) lines. The two spectra were essentially identical with the spectrum of AspAT at pH 6.9 (solid line).

At equilibrium,

$$\frac{[E_L][H_3^+O]}{[E_LH^+][H_2O]} = K_1\frac{k_2}{k_1} \qquad (5)$$

$$\frac{[E_L][H_2O]}{[E_LH^+][OH^-]} = \frac{1}{K_4}\frac{k_4}{k_3} \qquad (6)$$

The acid dissociation constant K_a is therefore expressed using

[4] A more simplified mechanism which assumes direct association of $H_3{}^+O$ and OH^- with the Schiff base is expressed by the following equations:

$$E_L + H_3{}^+O \overset{k_1^\circ}{\underset{k_2}{\rightleftharpoons}} E_LH^+ + H_2O$$

$$E_L + H_2O \overset{k_3}{\underset{k_4^\circ}{\rightleftharpoons}} E_LH^+ + OH^-$$

This can be considered to be the extreme case of eqs 3 and 4 in which k_1, K_1, k_4, and K_4 have infinite values. k_1° and k_4° are equal to k_1/K_1 and k_4/K_4, respectively. Equation 9 is then simplified as follows:

$$k_{app} = k_1^\circ \times 10^{-pH} + k_4^\circ \times 10^{pH-14} + k_1^\circ \times 10^{-pK_a} + k_4^\circ \times 10^{pK_a-14}$$

Fitting the results in Figure 4 to this equation, however, showed positive deviations of the theoretical values from the experimental values at acidic and basic limbs (data not shown). Therefore, the two-step mechanism described in the text (eqs 3 and 4) can explain more satisfactorily the experimental results.

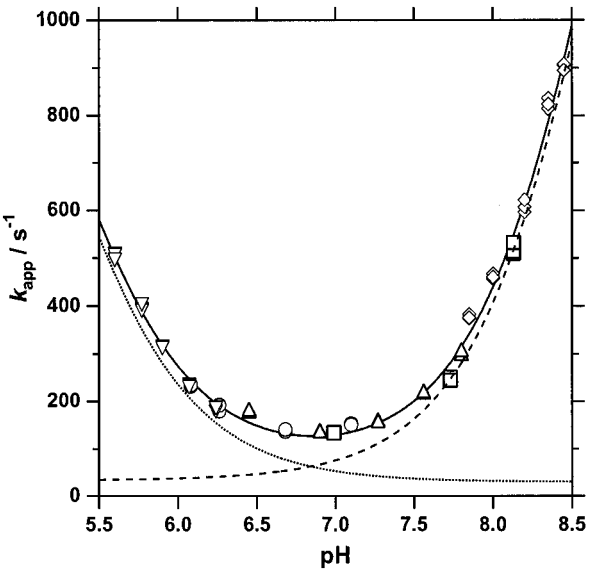

FIGURE 4: Plot of the apparent rate constant (k_{app}) for the exponential spectral change induced by pH jump/drop on the final pH value of the solution. Circles: Mixed MH buffer (pH 5.6, containing AspAT) with MH buffers with higher pH. Diamonds: Mixed MH buffer (pH 7.5, containing AspAT) with HT buffers with higher pH. Squares: Mixed HT buffer (pH 9.0, containing AspAT) with MH buffers with lower pH. Triangles: Mixed MH buffer (pH 8.0, containing AspAT) with MH buffers with lower pH. Reversed triangles: Mixed MH buffer (pH 6.5, containing AspAT) with MH buffers with lower pH. A theoretical line was drawn using eq 9. Dotted line and dashed line represent the calculated values of k_E (eq 10) and k_{EH} (eq 11), respectively.

k_1, k_2, k_3, k_4, K_1, and K_4:

$$K_a = \frac{[E_L][H_3^+O]}{[E_LH^+]} = \frac{K_1 k_2 [H_2O]}{k_1} \quad (7)$$

$$K_a = \frac{10^{-14}[E_L]}{[E_LH^+][OH^-]} = \frac{10^{-14} k_4}{K_4 k_3 [H_2O]} \quad (8)$$

The apparent rate constant for the spectral change on pH jump is

$$k_{app} = k_1 \frac{[H_3^+O]}{K_1 + [H_3^+O]} + k_3[H_2O] + k_2[H_2O] + k_4 \frac{[OH^-]}{K_4 + [OH^-]}$$

$$= k_1 \frac{10^{-pH}}{K_1 + 10^{-pH}} + k_4 \frac{10^{pK_a - 14}}{K_4} + k_1 \frac{10^{-pK_a}}{K_1} + k_4 \frac{10^{pH-14}}{K_4 + 10^{pH-14}} \quad (9)$$

Equation 9 gave excellent fitting of the theoretical line to the experimental values (Figure 4, solid line). The kinetic parameters were obtained to be: $k_1 = 1680 \pm 340$ s^{-1}, $k_2[H_2O] = 33 \pm 2$ s^{-1}, $K_1 = (7.1 \pm 1.7) \times 10^{-6}$ M, $k_3[H_2O] = 30 \pm 1$ s^{-1}, $k_4 = 2870 \pm 260$ s^{-1}, and $K_4 = (6.7 \pm 0.8) \times 10^{-6}$ M. Equation 9 shows that k_{app} is a simple sum of the apparent rate constant for $E_L \rightarrow E_LH^+$ (first two terms) and that for $E_LH^+ \rightarrow E_L$ (second two terms). These rate constants, denoted as k_E and k_{EH}, respectively, are expressed as follows:

$$k_E = k_1 \frac{10^{-pH}}{K_1 + 10^{-pH}} + k_4 \frac{10^{pK_a - 14}}{K_4} \quad (10)$$

$$k_{EH} = k_1 \frac{10^{-pK_a}}{K_1} + k_4 \frac{10^{pH-14}}{K_4 + 10^{pH-14}} \quad (11)$$

The values of k_E and k_{EH} were calculated using the obtained values of the parameters and are drawn in Figure 4 (dotted and broken lines). As expected, k_E and k_{EH} contribute largely to k_{app} at low and high pH, respectively. These values are of great use when we analyze the pH dependency of the half-reaction as follows.

AspAT with Protonated PLP−Lys258 Schiff Base Reacts with the Dianionic Form of Aspartate. As has been indicated previously (*12*, *13*), E_L is in equilibrium with E_LH^+, and E_L reacts with the substrate (SH^+) to form the first Michaelis complex (E_L·SH^+). The proton on the substrate amino group moves to the Schiff base and the resultant second Michaelis complex (E_LH^+·S) undergoes transaldimination to form the external aldimine, E_3, and subsequently to E_M (eq 12).

$$\begin{array}{ccccccc} E_L & \overset{k_{+1}[SH^+]}{\underset{k_{-1}}{\rightleftharpoons}} & E_L \cdot SH^+ & & & & \\ k_E \uparrow\downarrow & k_{EH} & \uparrow\downarrow K & & & & \\ E_LH^+ & & E_LH^+ \cdot S & \overset{k_{+2}}{\underset{k_{-2}}{\rightleftharpoons}} & E_3 & \overset{k_{+3}}{\underset{k_{-3}}{\rightleftharpoons}} & E_4 \overset{K_m^{half,OA}}{\underset{\pm OA}{\rightleftharpoons}} E_M \end{array} \quad (12)$$

Assuming that E_L, E_L·SH^+, E_LH^+·S, and E_3 are in rapid equilibrium (*21*), we obtain the following equation of the apparent rate constant for the decrease in the absorbance at 430 nm (see Appendix):

$$k_{app,430} = {}^1/_2(k_{EH} + Xk_E + \alpha(1-X)k_{+3} + Yk_{-3}) - {}^1/_2[(-k_{EH} - Xk_E + \alpha(1-X)k_{+3} + Yk_{-3})^2 + 4Xk_E\alpha(1-X)k_{+3}]^{1/2} \quad (13)$$

where

$$X = \frac{(K_m^{half,Asp})_A}{(K_m^{half,Asp})_A + [SH^+]}$$

$$Y = \frac{2[\overline{OA}]}{K_m^{half,OA} + 2[\overline{OA}]}$$

$$\alpha = \frac{K_{eq}^{Asp-OA}(K_m^{half,Asp})_A}{K_m^{half,OA}} \frac{k_{-3}}{k_{+3}}$$

Here, $(K_m^{half,Asp})_A$ is expressed by the following equation and is almost equal to the K_m^{half} value for aspartate experimentally obtained at pH 8 (*18*):

$$(K_m^{half,Asp})_A = \frac{k_{-1}/k_{+1}}{1 + K(1 + k_{+2}/k_{-2})}$$

The equilibrium concentration of oxalacetate, which is formed in an equimolar amount together with E_M, is

calculated as follows:

$$[\overline{OA}] = \frac{k_{EH}K_{eq}^{Asp-OA}}{2(k_E + k_{EH})}\left(-[SH^+] + \sqrt{[SH^+]^2 + 4[E_t][SH^+]\frac{k_E + k_{EH}}{k_{EH}K_{eq}^{Asp-OA}}}\right) \quad (14)$$

where K_{eq}^{Asp-OA} is the equilibrium constant for the reaction $E_L + SH^+ \rightleftarrows E_M + OA$ and is related to the kinetic parameters in eq 12:

$$K_{eq}^{Asp-OA} = \frac{k_{+1}}{k_{-1}}K\frac{k_{+2}}{k_{-2}}\frac{k_{+3}}{k_{-3}}K_m^{half,OA}$$

We already know the values of the following kinetic parameters (*18*): $K_{eq}^{Asp-OA} = 0.0052$,$(K_m^{half,Asp})_A = 4.5$ mM, $K_m^{half,OA} = 0.035$ mM, $k_{+3} = 550$ s^{-1}, and $k_{-3} = 800$ s^{-1}. The values of k_E and k_{EH} can be determined from Figure 4 and eqs 10 and 11 to be 187 and 39 s^{-1} (pH 6.1), 63 and 63 s^{-1} (pH 6.8), 38 and 153 s^{-1} (pH 7.4), and 35 and 217 s^{-1} (pH 7.7), respectively. The value of $[SH^+]$ is almost equal to the total concentration of aspartate, because the experiments in Figure 2A were carried out below pH 7.7 and the pK_a for the α-amino group of aspartate is 9.6. The total enzyme concentration, $[E_t]$, is 28 μM. Therefore, theoretical lines could be drawn using eq 13 (Figure 2A, dotted lines). At low pH values, i.e., pH 6.1, the theoretical values matched well with the experimental values at low concentrations of aspartate, namely 1−2 mM. However, the experimental values deviated positively from the theoretical lines at increasing concentrations of aspartate. The difference in the observed and the theoretical $k_{app,430}$ values, defined as $k_{app,430}^{residual} = k_{app,430}^{observed} - k_{app,430}^{theoretical}$, became larger not only with increasing concentration of aspartate but also with increasing pH (Figure 2A). The increase in pH in this range (pH 6.1−7.7) increases the fraction of the unprotonated form of the α-amino group of aspartate. Therefore, we calculated the concentration of the dianionic form[5] of aspartate using pK_a = 9.6 of the α-amino group and plotted $k_{app,430}^{residual}$ against the concentration of the dianionic form of aspartate (Figure 2B). The plots of the data at different pH values merged to a single line. This indicates that $k_{app,430}^{residual}$ is determined by the concentration of the dianionic form of aspartate, irrespective of the pH value. That $k_{app,430}^{residual}$ is the apparent rate constant for the decrease in the concentration of E_LH^+ through route(s) other than that shown in eq 12 and that the value is dependent on the concentration of the dianionic form of aspartate strongly suggest that $k_{app,430}^{residual}$ reflects the reaction of E_LH^+ and the dianionic form of aspartate (S). Therefore, we consider the following scheme for the complete description of the reaction of AspAT with aspartate:

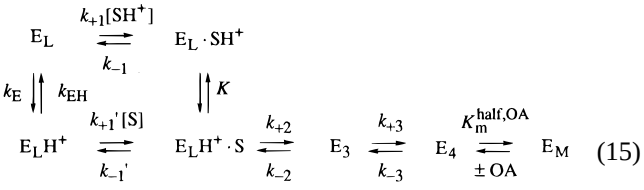

(15)

[5] The two carboxylate groups are dissociated, and the amino group is unprotonated.

The cycle in eq 15 yields the following relationship:

$$K = \frac{10^{-pK_a^{\alpha}}}{10^{-pK_a^{Schiff}}}\frac{k_{-1}}{k_{+1}}\frac{k_{+1}'}{k_{-1}'}$$

where pK_a^{Schiff} and pK_a^{α} are pK_a of the PLP−Lys258 Schiff base and that of the α-amino group of aspartate, respectively.

The apparent rate constant is described as follows (see Appendix):

$$k_{app,430} = \left\{k_{EH} + k_{+1}'[S] + Xk_E + \frac{10^{-pK_a^{\alpha}}}{10^{-pK_a^{Schiff}}}Xk_{+1}'[SH^+] + \alpha(1-X)k_{+3} + Yk_{-3} - \left[\left(-k_{EH} - k_{+1}'[S] - Xk_E - \frac{10^{-pK_a^{\alpha}}}{10^{-pK_a^{Schiff}}}Xk_{+1}'[SH^+] + \alpha(1-X)k_{+3} + Yk_{-3}\right)^2 + 4\left(Xk_E + \frac{10^{-pK_a^{\alpha}}}{10^{-pK_a^{Schiff}}}Xk_{+1}'[SH^+]\right)\alpha(1-X)k_{+3}\right]^{1/2}\right\}/2 \quad (16)$$

where X, Y, and α are the same as those used in eq 13. Although the equation has a complicated appearance, k_{+1}' is the only adjustable parameter. The theoretical curve provided an excellent fit to the experimental values, with the k_{+1}' value of (5.4 ± 0.2) × 10^6 M^{-1} s^{-1} (Figure 2A, solid lines). This supports the validity of the scheme expressed by eq 15. Scheme 1 is drawn based on eq 15. From now, we refer to $E_L + SH^+ \rightleftarrows E_L{\cdot}SH^+$ and $E_LH^+ + S \rightleftarrows E_LH^+{\cdot}S$ as route A and route B, respectively.

The $k_{app,430}^{residual}$ value showed a *linear* dependency on the concentration of the dianionic form of aspartate (S) up to 0.07 mM (Figure 2B). The slope was around 5.5 × 10^6 M^{-1} s^{-1}, which was in good agreement with the k_{+1}' value. This indicates that, for the direct conversion of E_LH^+ to E_M through route B, the bimolecular association step of S and E_LH^+ is rate-limiting at [S] < 0.07 mM, because of the limiting concentrations of the dianionic form of aspartate.

The plot in Figure 2B shows that the maximum value of $k_{app,430}^{residual}$ is about 800 s^{-1}. This value is almost equal to the maximum value of $k_{app,377}$ (Figure 2A). If the interconversion of $E_LH^+{\cdot}S$ and $E_L{\cdot}SH^+$ is slow compared to the rate of the transaldimination reaction $E_LH^+{\cdot}S \rightleftarrows E_3$, the maximum rate of the reaction from E_LH^+ to E_M should be greater than that of the reaction from E_L to E_M, because the association of E_LH^+ with S yields directly the reactive species $E_LH^+{\cdot}S$. The almost equal values indicate that the interconversion of $E_LH^+{\cdot}S$ and $E_L{\cdot}SH^+$ is rapid compared with the transaldimination process, $E_LH^+{\cdot}S \rightleftarrows E_3$.

Monoanionic Form of Aspartate and the Schiff-Base-Nonprotonated Form of AspAT Are Preferentially Formed from the Enzyme−Substrate Complex. During the course of the "reverse" reaction from E_M to E_L/E_LH^+, $E_LH^+{\cdot}S$ is formed from E_3 by transaldimination (Scheme 1). $E_LH^+{\cdot}S$ can either undergo dissociation to form $E_LH^+ + S$ (route B) or rapidly equilibrate with $E_L{\cdot}SH^+$, then dissociate into $E_L + SH^+$ (route A). In order to find which route is preferred, we analyzed the spectral transitions on the reaction of E_M with oxalacetate. The steps except for the interconversion

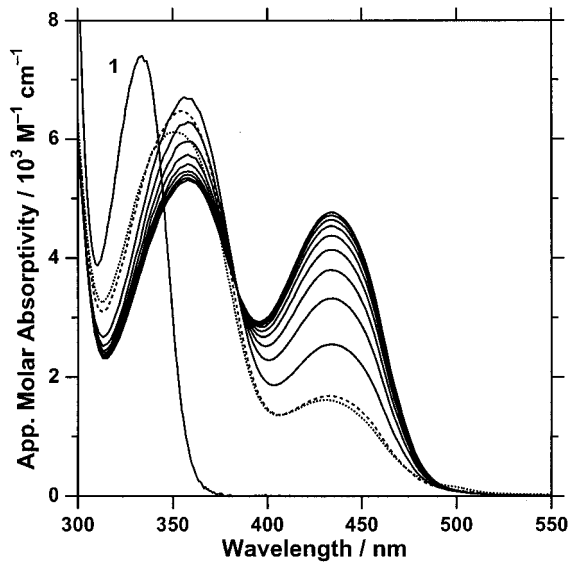

FIGURE 5: Time-dependent absorption change of AspAT on reaction with oxalacetate at pH 6.8, 298K. The PMP form of AspAT (25 μM; Curve 1) was reacted with 1 mM oxalacetate in MH buffer, pH 6.8. The spectra were taken in the same way as in Figure 4. Dotted line, $t = 2.3$ ms. Dashed line, $t = 3.64$ ms. The spectra at $t = 6.2$, 8.76, 11.32, 13.88, 16.44, 19.0, 21.56, and 24.12 ms (from bottom to top of the 430-nm absorption band) showed an isosbestic point at 385 nm. For these spectra (after $t = 6.2$ ms), the absorption at 430 nm gradually increased exponentially ($k_{app} = 130$ s^{-1}) with a concomitant decrease in absorbance at 358 nm. Absorption due to oxalacetate was subtracted from each spectrum.

of E_L and E_LH^+ and the 1,3-prototropic shift (expressed by k_{+3} and k_{-3}) are regarded to proceed rapidly. In addition, the equilibrium shift of the half-reaction by ~180 toward the PLP form of the enzyme (*18*) enabled us to consider that the conversion from E_M to E_L/E_LH^+ is essentially irreversible. Therefore, the reaction from E_M in the presence of a saturating concentration of oxalacetate is expressed by the following equation:

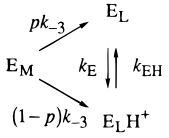

(17)

Here p denotes the proportion of the reactions to yield E_L in the total reactions from E_M to E_L/E_LH^+. The absorption change is expressed as follows (see Appendix):

$$\frac{A}{[E_t]} = \frac{k_{EH}}{k_E + k_{EH}}\epsilon_{E_L} + \frac{k_E}{k_E + k_{EH}}\epsilon_{E_LH^+} + \left[\epsilon_{E_M} - \frac{pk_{-3} - k_{EH}}{k_{-3} - k_E - k_{EH}}\epsilon_{E_L} - \frac{(1-p)k_{-3} - k_E}{k_{-3} - k_E - k_{EH}}\epsilon_{E_LH^+}\right] \times \exp(-k_{-3}t) + (\epsilon_{E_L} - \epsilon_{E_LH^+})\frac{pk_{-3}k_E - (1-p)k_{-3}k_{EH}}{(k_{-3} - k_E - k_{EH})(k_E + k_{EH})} \times \exp[-(k_E + k_{EH})t] \quad (18)$$

As shown in Figure 5, there were a rapid decrease in intensity of the 333-nm absorption band and increases in intensity of the 358- and 430-nm absorption bands, corresponding to the third term of eq 18. After $t = 6.2$ ms, the spectrum changed monoexponentially, as indicated by the presence of the isosbestic point at 385 nm (Figure 5), and this corresponded to the fourth term of eq 18. Because we carried out the experiment at pH 6.8, where the interconversion of E_L and E_LH^+ is slowest (Figure 4), we could well separate the two exponential changes. Therefore, if we consider the time-resolved spectra after $t = 6.2$ ms, where the first exponential change is over, we can neglect the third term of eq 18. Because E_M and E_L has no absorption at 430 nm, the time-dependent absorption change at 430 nm after $t = 6.2$ ms is expressed as follows:

$$\frac{A_{430}}{[E_t]} = \left\{\frac{k_E}{k_E + k_{EH}} - \frac{pk_{-3}k_E - (1-p)k_{-3}k_{EH}}{(k_{-3} - k_E - k_{EH})(k_E + k_{EH})}\exp[-(k_E + k_{EH})t]\right\}\epsilon_{E_LH^+,430} \quad (19)$$

Using the values $k_{-3} = 800$ s^{-1}, $k_E = 63$ s^{-1} (pH 6.8), $k_{EH} = 63$ s^{-1} (pH 6.8), and $A_{430}/([E_t]\epsilon_{E_LH^+,430}) = 0.268$ at $t = 6.2$ ms, the value of p is calculated to be 0.93. Therefore, we can conclude that $E_L + SH^+$ is preferentially formed by the reverse reaction. An experiment using 1 mM 2-oxoglutarate in place of 1 mM oxalacetate gave a similar result with $p = 0.96$.

DISCUSSION

Kinetic Resolution of the Two Routes to the Enzyme−Substrate Complex. The present study showed that the interconversion of E_L and E_LH^+, i.e., protonation/deprotonation of the PLP−Lys258 Schiff base of AspAT, is unexpectedly slow, with a minimum value of 126 s^{-1} at pH 6.8. Due to this slow equilibrium and to the relatively slow bimolecular association process of route B as is discussed below, the disappearance of E_L and that of E_LH^+ on reaction with aspartate could be kinetically resolved. The disappearance of E_L was essentially pH independent, reflecting the association of E_L and the monoanionic form of aspartate, SH^+, which is the dominant species within the pH range used in this study (route A). On the other hand, the disappearance of E_LH^+ was clearly dependent on the concentration of the dianionic form of aspartate, S, which increases with increasing pH (Figure 2B). This indicated that E_LH^+ and S associate (route B) and undergo further reactions. The two routes merge into the same Michaelis complex, which is an equilibrium mixture of $E_L{\cdot}SH^+$ and $E_LH^+{\cdot}S$. Thus, the present study has just added route B to the classical mechanism (Scheme 1).

It is, however, important to note that the two routes are intrinsically "kinetically equivalent" mechanisms; that is, they form a set of mechanisms that usually cannot be distinguished by examining the pH dependency of the reaction (*16*). The principle is shown in Figure 6, where the pH dependence of the fraction of the active form of the enzyme (f_E), that of the active form of the substrate (f_S), and that of the product $f_E f_S$ are shown. The left panels (mechanism A) and right panels (mechanism B) were drawn based on assumptions that only route A and route B are involved, respectively. The pK_a of the substrate α-amino group (pK_a^{α}) was taken as 9.6, and that of the Schiff base (pK_a^{Schiff}) as 6.8 (upper panels) and 12 (lower panels). Both mechanism A and mechanism B showed an identical shape of the log($f_E f_S$)−pH profile. The presence of a thermodynamic cycle comprising $E_L + SH^+$, $E_L{\cdot}SH^+$, $E_LH^+ + S$, and $E_LH^+{\cdot}S$ indicates that the pH-independent k_{cat}/K_m value for mechanism B should be $10(pK_a^{\alpha} - pK_a^{Schiff})$ times larger than that for mechanism A.

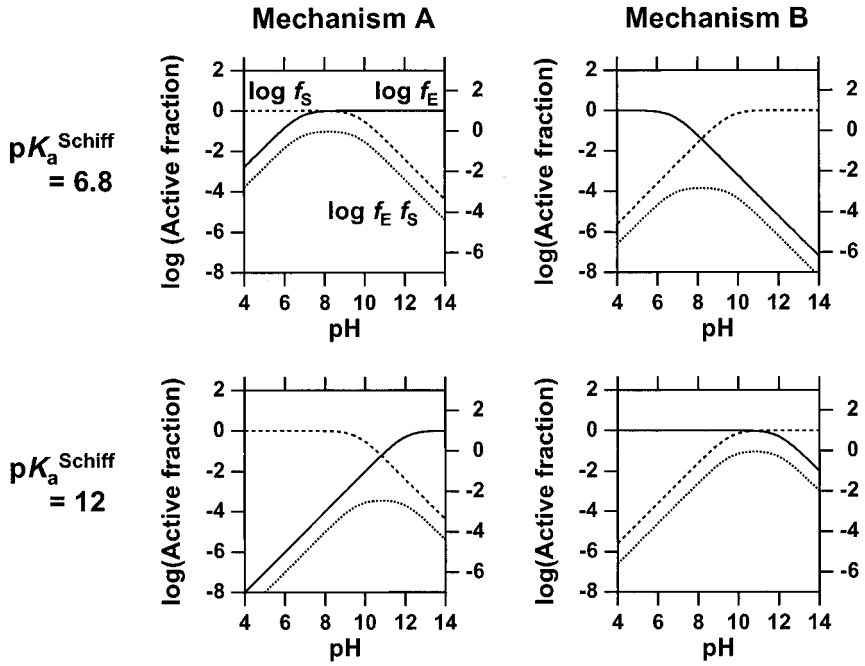

FIGURE 6: Diagrams to show the pH dependent distribution of active reactants. Logarithm of the fraction of active enzyme (log f_E, solid lines), that of active substrate (log f_S, dashed lines), and the sum of these two (log f_E + log f_S = log($f_E f_S$), dotted lines; the values are shown on the right axes which were offset by 1 for clarity) are shown. Upper panels: The theoretical lines are drawn based on the assumption that the association of the enzyme and the substrate proceeds through only route A (mechanism A) and only route B (mechanism B). The pK_a values of the Schiff base and the α-amino group of the substrate are 6.8 and 9.6, respectively. Lower panels: Same as upper panels except for that the pK_a of the Schiff base is 12.

This compensates the low $f_E f_S$ value of mechanism B, which is $10^{(pK_a^{\alpha} - pK_a^{Schiff})}$ times smaller than that of mechanism A, and therefore the two mechanisms are expected to have identical k_{cat}/K_m values with identical pH dependency. These considerations indicate that even if the interconversion of E_L and E_LH^+ is slow, the two mechanisms cannot be distinguished kinetically unless there are additional features that lead to differences in the kinetic behavior between the two mechanisms. In AspAT, because the $f_E f_S$ value of mechanism B is $10^{2.8}$ times smaller than that of mechanism A, the bimolecular association rate constant for mechanism B must be larger than $(k_{cat}/K_m)_A \times 10^{2.8} = 7.9 \times 10^7$ M^{-1} s^{-1} in order for mechanism B to show kinetic behavior identical to that of mechanism A. The fact that this exceeds the k_{+1}' value (5.4×10^6 M^{-1} s^{-1}) can be considered to be responsible for the successful resolution of the two routes in this study. This at the same time indicates that route B cannot be the sole route of the association process of aspartate and AspAT.

The relatively small value of 5.4×10^6 M^{-1} s^{-1} for the bimolecular association constant for route B, compared with the value 10^8 M^{-1} s^{-1} for route A (*21*), was an unexpected finding. The reason for this difference is not clear at present. It has been argued that the association of an enzyme with a substrate molecule at a rate constant approaching the diffusion-controlled limit (10^8 M^{-1} s^{-1}) is assisted by electrostatic guiding of a polar substrate to the enzyme's active site, and in the case of AspAT, the interaction between the positively charged ammonium group of SH^+ and the negatively charged 3′-O of PLP of E_L has been considered to increase the efficiency of the binding of SH^+ to E_L (*12*). The interaction is absent in the binding process of S to E_LH^+, and we may reasonably consider that this difference is the reason for the relatively low value of k_{+1}' compared with k_{+1}.

Advantage of Route A over Route B in the Catalytic Reaction of AspAT. The two routes to the enzyme−substrate complex have been successfully resolved; therefore, the next intriguing question is the extent of contribution of each route in actual catalysis. In the half-reaction, according to the calculation using eqs 13 and 16, the rate of conversion of E_LH^+ to E_M through route B is 190 s^{-1}, and that through route A is 160 s^{-1}, at pH 7.4 and with an aspartate concentration of 5 mM. The rate of conversion from E_L to E_M with 5 mM aspartate is calculated to be 290 s^{-1} (*18*). At pH 7.4, E_LH^+ occupies 20% of the PLP form of the enzyme. Therefore, the contribution of route B to the catalytic reaction is calculated to be $(0.20 \times 190)/(0.80 \times 290 + 0.20 \times (190 + 160)) = 13\%$. Thus, the contribution of route B to the first half-reaction of AspAT (eq 1) with aspartate under physiological conditions is less than the fraction of the Schiff-base-protonated species, E_LH^+. Again, the disadvantage of route B is because this association process becomes rate determining in the transition from E_LH^+ to E_M due to the limiting concentration of S. In accordance with this, the reaction rate through route B approaches that through route A at higher concentrations of aspartate (over 0.12 mM of the dianionic form; Figure 2B), where bimolecular association is not rate determining.

In the overall reaction, the PLP form of enzyme is regenerated from the reaction of E_M with an oxo acid substrate. The PLP form is preferentially formed in the E_L form, not in the E_LH^+ form (Figure 5). The overall ping-pong Bi Bi reaction is therefore expressed as follows:

$$\begin{array}{ccccccccc} E_L & \underset{k_{-1}}{\overset{k_{+1}[SH^+]}{\rightleftharpoons}} & E_L \cdot SH^+ & & & & & & \\ k_E \uparrow\downarrow k_{EH^+} & & \downarrow\uparrow K & & & & & & \\ E_LH^+ & \underset{k_{-1}'}{\overset{k_{+1}'[S]}{\rightleftharpoons}} & E_LH^+ \cdot S & \underset{k_{-2}}{\overset{k_{+2}}{\rightleftharpoons}} & E_3 \cdots E_{n-1} & \underset{k_{-(n-1)}}{\overset{k_{+(n-1)}}{\rightleftharpoons}} & E_n & \xrightarrow{k_{+n}} & E_L \end{array} \quad (20)$$

Here, the Michaelis complex formed from E_M and the oxo acid substrate was simply expressed as E_n. The association/dissociation of SH^+ and E_L is rapid (*21*). The interconversion of $E_L{\cdot}SH^+ \rightleftarrows E_LH^+{\cdot}S$ is rapid as compared with the transaldimination step, $E_LH^+{\cdot}S \rightleftarrows E_3$ (see Results). Therefore, E_L, $E_L{\cdot}SH^+$, and $E_LH^+{\cdot}S$ are considered to be in rapid equilibrium in the steady-state reaction. This indicates a value exists for the concentration of E_LH^+ that enables E_LH^+ to be in equilibrium with E_L and $E_LH^+{\cdot}S$ simultaneously. Accordingly, we can expect that although the interconversion of $E_L \rightleftarrows E_LH^+$ and $E_LH^+ \rightleftarrows E_LH^+{\cdot}S$ is slow, the concentration of E_LH^+ can reach such an "equilibrium" value. In such a circumstance, the rate of the overall reaction can be expressed as follows (see Appendix):

$$\frac{[E_t]}{\nu} = \left(\frac{k_{-1}'}{k_{+1}'}\right)\left(\frac{K_a^{Schiff} + [H^+]}{[H^+]}\right)\left(\frac{K_a^{\alpha} + [H^+]}{K_a^{\alpha}}\right)\left(\frac{1}{k_{+2}} + \frac{k_{-2}}{k_{+2}}\frac{1}{k_{+3}} + ... + \frac{k_{-2}}{k_{+2}}...\frac{k_{-(n-1)}}{k_{+(n-1)}}\frac{1}{k_{+n}}\right)\frac{1}{[S_t]} + \left(1 + \frac{K_a^{Schiff}}{K_a^{\alpha}}\frac{k_{+1}}{k_{-1}}\frac{k_{-1}'}{k_{+1}'}\right)\left(\frac{1}{k_{+2}} + \frac{k_{-2}}{k_{+2}}\frac{1}{k_{+3}} + ... + \frac{k_{-2}}{k_{+2}}...\frac{k_{-(n-1)}}{k_{+(n-1)}}\frac{1}{k_{+n}}\right) + \sum_{i=3}^{n}\left(\frac{1}{k_{+i}} + \frac{k_{-i}}{k_{+i}}\frac{1}{k_{+(i+1)}} + ... + \frac{k_{-i}}{k_{+i}}...\frac{k_{-(n-1)}}{k_{+(n-1)}}\frac{1}{k_{+n}}\right) \quad (21)$$

Therefore, $k_{cat}^{overall}/K_m^{overall}$ shows the pH dependency as follows:

$$\log(k_{cat}^{overall}/K_m^{overall}) = \log(k_{cat}^{overall}/K_m^{overall})_{max} + \log\frac{10^{-pH}}{K_a^{Schiff} + 10^{-pH}} + \log\frac{K_a^{\alpha}}{K_a^{\alpha} + 10^{-pH}} \quad (22)$$

which is exactly the equation that describes the bell-shaped pH profile of $\log(k_{cat}/K_m)$ for aspartate (*10*).

The flow from E_L to $E_LH^+{\cdot}S$ proceeds via either $E_L \rightleftarrows E_L{\cdot}SH^+ \rightleftarrows E_LH^+{\cdot}S$ or $E_L \rightleftarrows E_LH^+ \rightleftarrows E_LH^+{\cdot}S$, the latter of which includes route B. In the former process, the rate constant for $E_L \rightarrow E_L{\cdot}SH^+$ is larger than 10^8 M^{-1} s^{-1} (*21*). The rate constant for $E_L{\cdot}SH^+ \rightarrow E_LH^+{\cdot}S$ is not known, but must be larger than the rate constant for the transaldimination step, which is estimated to be about 10^4 s^{-1} from the studies on model compounds (*22*). In the latter process, the step $E_L \rightarrow E_LH^+$ is obviously rate-determining and is below 100 s^{-1} at neutral pH (k_E, Figure 4). Therefore, route B is estimated to contribute less than 1% to the overall catalytic reaction. As described above, the PLP form of the enzyme is generated in the E_L form and not in the E_LH^+ form by the reaction of E_M with oxo acids. Accordingly, route B requires conversion of E_L to E_LH^+ before reacting with the substrate, which is slow at neutral pH values. Therefore, even in the presence of a high concentration of aspartate, the contribution of route B to the overall catalytic rate is not significant because of the slow, rate-determining conversion of E_L to E_LH^+.

Implications for the Reaction Mechanisms of PLP Enzymes. The PLP−Lys Schiff base of AspAT has an unusually low pK_a value (6.8) compared with other PLP-dependent enzymes (generally above 11). Although the exact mechanism that decreases the Schiff-base pK_a value is yet to be determined, this low pK_a value is obviously important for the enzyme to be effective at neutral pH (Figure 6). Mechanism B was less advantageous than mechanism A, due to the low value of $f_E f_S$ that makes the bimolecular association process rate determining (see above discussions). In other PLP enzymes that have higher Schiff base pK_a values, the pH profiles of $f_E f_S$ will be such as those shown in the lower panels of Figure 6, with pH optimum shifted upward compared with that of the profiles of AspAT. Because the Schiff base pK_a was taken as 12, $f_E f_S$ of mechanism B is $10^{(12-9.6)} = 10^{2.4}$ times larger than that of mechanism A. Assuming that the bimolecular association rate constants are the same as those of AspAT, we can expect that the upper limit of the pH-independent value of k_{cat}/K_m is $10^8/10^{2.4} = 4 \times 10^5$ M^{-1} s^{-1} for mechanism A, and 5.4×10^6 M^{-1} s^{-1} for mechanism B, respectively. At lower pH values, these values decrease by 10^2 (pH 8.0)- to 10^3 (pH 7.0)-fold (Figure 6). The k_{cat}/K_m values of most PLP enzymes fall in the range of 10^3−10^5 M^{-1} s^{-1}, which were generally measured between pH 7 and 10. Therefore, it seems likely that either mechanism A or mechanism B, or both, can be applied to the catalytic mechanism of most PLP enzymes. However, we must take into account the form of the enzyme regenerated after a cycle of catalysis. In aminotransferases, the second half-reaction regenerates the PLP form of the enzyme and the amino acid product from the PMP form of the enzyme and the oxo acid substrate. In decarboxylases, the amine product and the PLP form of the enzyme are formed. All other PLP enzymes regenerate the amino or imino acid product and the PLP form of the enzyme. The second half-reaction of AspAT showed that the E_L form of the enzyme is regenerated. This was interpreted to be due to the shift in equilibrium of $E_L + SH^+ \rightleftarrows E_LH^+ + S$ toward $E_L + SH^+$ by a factor of $10^{2.8}$. Similar considerations on the other PLP enzymes with higher Schiff-base pK_a suggest that E_LH^+ is preferentially formed in these enzymes. If this is the case, mechanism A requires the conversion of E_LH^+ to E_L before reacting with the substrate. The rate of this reaction is greater than 100 s^{-1} at pH values higher than 7.0 and approaches 1000 s^{-1} at pH 8.5 (Figure 4); these values are higher than the k_{cat} values of most PLP enzymes. Therefore, we still cannot rule out the contribution of route A to the catalytic mechanism of PLP enzymes other than AspAT. Detailed kinetic analyses, especially studies on the pH dependence of kinetic parameters such as k_{cat}/K_m and the bimolecular association rate constant for the enzyme and the substrate, are required to clarify the contribution of the two routes in these enzymes. Recent investigations on *O*-acetylserine sulfhydrylase by Cook, Schnackerz, and colleagues (*23*, *24*) showed that the α-amino group deprotonated form of the substrate binds to the Schiff-base-protonated form of the enzyme.

Another important point to be addressed is the possibility of the presence of mechanism(s) other than route A and route B for association of PLP enzymes and substrates. In the present study, we did not take into account the $E_LH^+{\cdot}SH^+$ and the $E_L{\cdot}S$ structures. This is because the AspAT−2-

methylaspartate complex shows a pH-independent spectrum, and therefore coexistence of $E_LH^+ \cdot SH^+$ and $E_L \cdot SH^+$ or $E_LH^+ \cdot S$ and $E_L \cdot S$ is not likely to occur (*15*). In the catalytic reaction of other PLP enzymes with high Schiff base pK_a values, E_LH^+ and SH^+ are the main species present in the solution. If E_LH^+ and SH^+ undergo association, the resultant $E_LH^+ \cdot SH^+$ structure must be deprotonated to $E_LH^+ \cdot S$ before it undergoes transaldimination. It is possible to consider a hypothetical base that locates in the active site and accepts the proton from the Schiff base. In ornithine decarboxylase, a histidine residue is found to stack with the pyridine ring of PLP and occupies a position that can interact with the α-amino group of the substrate (*25*). This histidine residue might be considered to be the base, although no further analysis has been performed to test the hypothesis. In the other PLP enzymes whose three-dimensional structures have been solved, i.e., tryptophan synthase (*26*), D-amino acid aminotransferase (*27*), branched-chain amino acid aminotransferase (*28*), dialkylglycine decarboxylase (*29*), and tyrosine phenol-lyase (*30*, *31*), there is no such base located near PLP that can interact with the α-amino group of substrate amino acids. Therefore, we consider that association of an enzyme with a substrate through route A or route B is a mechanism that is used by many, if not all, PLP enzymes.

Conclusions. The transient kinetics of the reaction of AspAT with aspartate at low pH confirmed the classical route to the ES complex in which the Schiff-base-unprotonated form of AspAT associates with the monoanionic form of aspartate. In addition, a second route in which the Schiff-base-protonated form of AspAT associates with the dianionic form of aspartate could be kinetically separated from the first route. The reaction of oxalacetate and the PMP form of AspAT preferentially formed the Schiff-base-unprotonated species of the PLP form enzyme. Therefore, the second route contributes little to the overall catalytic reaction due to the slow conversion of the Schiff-base-unprotonated enzyme to the protonated enzyme. However, the discovery of the binary association mode of AspAT and aspartate suggests that this mode may also be applicable to the reaction mechanism of other PLP enzymes having high Schiff base pK_a values, and in these enzymes, the second route may contribute largely to the function of the enzyme.

APPENDIX

Derivations of Eqs 13 and 16. Equation 12 can be reduced to the following equation if we assume that E_L, $E_L \cdot SH^+$, and $E_LH^+ \cdot S$ and E_3 are in rapid equilibrium:

$$E_LH^+ \underset{k_E^\circ}{\overset{k_{EH}}{\rightleftharpoons}} E^\circ \underset{k_{-3}^\circ}{\overset{k_{+3}^\circ}{\rightleftharpoons}} E_M \tag{1a}$$

where

$$k_E^\circ = 1/\left\{1 + \frac{k_{+1}[SH^+]}{k_{-1}} + \frac{k_{+1}[SH^+]}{k_{-1}}K + \frac{k_{+1}[SH^+]}{k_{-1}}K\frac{k_{+2}}{k_{-2}}\right\}k_E = Xk_E \tag{2a}$$

$$k_{+3}^\circ = \left\{\frac{k_{+1}[SH^+]}{k_{-1}}K\frac{k_{+2}}{k_{-2}}\right\}/\left\{1 + \frac{k_{+1}[SH^+]}{k_{-1}} + \frac{k_{+1}[SH^+]}{k_{-1}}K + \frac{k_{+1}[SH^+]}{k_{-1}}K\frac{k_{+2}}{k_{-2}}\right\}k_{+3} = \alpha(1 - X)k_{+3} \tag{3a}$$

$$k_{-3}^\circ = \frac{2[\overline{OA}]}{K_m^{half,OA} + 2[\overline{OA}]}k_{-3} = Yk_{-3} \tag{4a}$$

Here, the rate constant for the step from E_M to E°, k_{-3}°, is approximated using $K_m^{half,OA}$ and the equilibrium concentration of oxalacetate (*18*).

The concentrations of E_LH^+ and E_L are expressed using their equilibrium concentrations and the deviations to be

$$[E_L] = [\overline{E_L}] + \Delta[E_L]$$

$$[E_LH^+] = [\overline{E_LH^+}] + \Delta[E_LH^+]$$

Using this expression, the following equations are obtained for eq 1a:

$$-\frac{\delta\Delta[E_LH^+]}{\delta t} = k_{EH}\Delta[E_LH^+] - k_E^\circ\Delta[E^\circ] \tag{5a}$$

$$-\frac{\delta\Delta[E^\circ]}{\delta t} = (-k_{EH} + k_{-3}^\circ)\Delta[E_LH^+] + (k_E^\circ + k_{+3}^\circ + k_{-3}^\circ)\Delta[E^\circ] \tag{6a}$$

Solving eqs 5a and 6a yields eq 13, which describes the apparent rate constant for the slower phase of the spectral changes.

Similarly, eq 15 can be reduced to the following equation if we assume that E_L, $E_L \cdot SH^+$, and $E_LH^+ \cdot S$ and E_3 are in rapid equilibrium:

$$E_LH^+ \underset{k_E^*}{\overset{k_{EH} + k_{+1}'[S]}{\rightleftharpoons}} E^\circ \underset{k_{-3}^\circ}{\overset{k_{+3}^\circ}{\rightleftharpoons}} E_M \tag{7a}$$

where

$$k_E^* = \left(\frac{k_{+1}[SH^+]}{k_{-1}}K\right)/\left\{1 + \frac{k_{+1}[SH^+]}{k_{-1}} + \frac{k_{+1}[SH^+]}{k_{-1}}K + \frac{k_{+1}[SH^+]}{k_{-1}}K\frac{k_{+2}}{k_{-2}}\right\}k_{-1}' + k_E^\circ = Xk_E + \frac{k_{+1}}{k_{-1}}KXk_{-1}'[SH^+] \tag{8a}$$

The following equations are obtained:

$$-\frac{\delta\Delta[E_LH^+]}{\delta t} = (k_{EH} + k_{+1}'[S])\Delta[E_LH^+] - k_E^*\Delta[E^\circ] \quad (9a)$$

$$-\frac{\delta\Delta[E^\circ]}{\delta t} = (-k_{EH} - k_{+1}'[S] + k_{-3}^\circ)\Delta[E_LH^+] + (k_E^* + k_{+3}^\circ + k_{-3}^\circ)\Delta[E^\circ] \quad (10a)$$

Solving eqs 9a and 10a yields the following equation that describes the apparent rate constant for the slower phase of the spectral changes:

$$k_{app,430} = \left\{k_{EH} + k_{+1}'[S] + Xk_E + \frac{k_{+1}}{k_{-1}}KXk_{-1}'[SH^+] + \alpha(1-X)k_{+3} + Yk_{-3} - \left[\left(-k_{EH} - k_{+1}'[S] - Xk_E - \frac{k_{+1}}{k_{-1}}KXk_{-1}'[SH^+] + \alpha(1-X)k_{+3} + Yk_{-3}\right)^2 + 4\left(Xk_E + \frac{k_{+1}}{k_{-1}}KXk_{-1}'[SH^+]\right)\alpha(1-X)k_{+3}\right]^{1/2}\right\}/2 \quad (11a)$$

Using the relationship

$$K = \left(\frac{10^{-pK_a^\alpha}}{10^{-pK_a^{Schiff}}}\right)\left(\frac{k_{-1}}{k_{+1}}\right)\left(\frac{k_{+1}'}{k_{-1}'}\right)$$

we can rearrange eq 11a to eq 16.

Derivation of Eq 18. From eq 17, the following differential equations are derived.

$$-\frac{\delta[E_L]}{\delta t} = -pk_{-3}[E_M] + k_E[E_L] - k_{EH}[E_LH^+] \quad (12a)$$

$$-\frac{\delta[E_LH^+]}{\delta t} = -(1-p)k_{-3}[E_M] - k_E[E_L] + k_{EH}[E_LH^+] \quad (13a)$$

At $t = 0$, $[E_M] = [E_t]$ and $[E_L] = [E_LH^+] = 0$. At $t = \infty$, $[E_M] = 0$, $[E_L] = k_{EH}/(k_E + k_{EH})[E_t]$, and $[E_LH^+] = k_E/(k_E + k_{EH})[E_t]$. Equations 12a and 13a are solved under these conditions to yield

$$\frac{[E_L]}{[E_t]} = \frac{k_{EH}}{k_E + k_{EH}} - \frac{pk_{-3} - k_{EH}}{k_{-3} - (k_E + k_{EH})}\exp(-k_{-3}t) + \frac{pk_{-3}k_E - (1-p)k_{-3}k_{EH}}{(k_{-3} - k_E - k_{EH})(k_E + k_{EH})}\exp[-(k_E + k_{EH})t] \quad (14a)$$

$$\frac{[E_LH^+]}{[E_t]} = \frac{k_E}{k_E + k_{EH}} - \frac{(1-p)k_{-3} - k_E}{k_{-3} - (k_E + k_{EH})}\exp(-k_{-3}t) - \frac{pk_{-3}k_E - (1-p)k_{-3}k_{EH}}{(k_{-3} - k_E - k_{EH})(k_E + k_{EH})}\exp[-(k_E + k_{EH})t] \quad (15a)$$

Using eqs 14a and 15a and the molar absorptivities of E_L, E_LH^+, and E_M, eq 18 is obtained.

Derivation of Eq 23. For the scheme of the overall reaction (eq 20), we can obtain the following equations on the assumption that E_L, E_LH^+, $E_L{\cdot}SH^+$, and $E_LH^+{\cdot}S$ are in equilibrium:

$$k_{+1}[SH^+][E_L] = k_{-1}[E_L{\cdot}SH^+] \quad (16a)$$

$$K_a^{Schiff} = \frac{[E_L][H^+]}{[E_LH^+]} \quad (17a)$$

$$k_{+1}'[S][E_LH^+] = k_{-1}'[E_LH^+{\cdot}S] \quad (18a)$$

$$K_a^\alpha = \frac{[H^+][S]}{[SH^+]} \quad (19a)$$

Using these relationships, we obtain

$$\begin{aligned}&[E_L] + [E_L{\cdot}SH^+] + [E_LH^+] + [E_LH^+{\cdot}S]\\ &= \left\{\left[\left(1 + \frac{k_{+1}}{k_{-1}}[SH^+]\right)\frac{K_a^{Schiff}}{[H^+]} + 1\right]\frac{k_{-1}'}{k_{+1}'[S]} + 1\right\}[E_LH^+{\cdot}S]\\ &= \left\{\left[\left(1 + \frac{k_{+1}}{k_{-1}}\frac{[H^+]}{K_a^\alpha + [H^+]}[S_t]\right)\frac{K_a^{Schiff}}{[H^+]} + 1\right]\times \frac{k_{-1}'}{k_{+1}'}\frac{K_a^\alpha + [H^+]}{K_a^\alpha}\frac{1}{[S_t]} + 1\right\}[E_LH^+{\cdot}S]\\ &= \left\{\frac{k_{-1}'}{k_{+1}'}\frac{K_a^{Schiff} + [H^+]}{[H^+]}\frac{K_a^\alpha + [H^+]}{K_a^\alpha}\frac{1}{[S_t]} + \frac{K_a^{Schiff}}{K_a^\alpha}\frac{k_{+1}}{k_{-1}}\frac{k_{-1}'}{k_{+1}'} + 1\right\}[E_LH^+{\cdot}S]\end{aligned} \quad (20a)$$

Therefore, eq 20 can be reduced to the following equation:

$$E_2^\circ \underset{k_{-2}}{\overset{k_{+2}^\circ}{\rightleftarrows}} E_3 \ldots E_{n-1} \underset{k_{-(n-1)}}{\overset{k_{+(n-1)}}{\rightleftarrows}} E_n \xrightarrow{k_{+n}} E_2^\circ \quad (21a)$$

where

$$k_{+2}^\circ = 1/\left\{\frac{k_{-1}'}{k_{+1}'}\frac{K_a^{Schiff} + [H^+]}{[H^+]}\frac{K_a^\alpha + [H^+]}{K_a^\alpha}\frac{1}{[S_t]} + \frac{K_a^{Schiff}}{K_a^\alpha}\frac{k_{+1}}{k_{-1}}\frac{k_{-1}'}{k_{+1}'} + 1\right\}k_{+2} \quad (22a)$$

Using the equation for the steady-state kinetics for the overall catalytic reaction (*14*), the rate for the overall reaction eq 20 is expressed by eq 21.

REFERENCES

1. Arnone, A., Rogers, P. H., Hyde, C. C., Briley, P. D., Metzler, C. M., and Metzler, D. E. (1985) in *Transaminases* (Christen, P., and Metzler, D. E., Eds.) pp 138−154, John Wiley & Sons, New York.
2. McPhalen, C. A., Vincent, M. G., and Jansonius, J. N. (1992) *J. Mol. Biol. 225*, 495−517.
3. Malashkevich, V. N., Toney, M. D., and Jansonius, J. N. (1993) *Biochemistry 32*, 13451−13462.
4. Malashkevich, V. N., Strokopytov, B. V., Borisov, V. V., Dauter, Z. Wilson, K. S., and Torchinsky, Y. M. (1995) *J. Mol. Biol. 247*, 111−124.
5. Jäger, J., Moser, M., Sauder, U., and Jansonius, J. N. (1994) *J. Mol. Biol. 239*, 285−305.

6. Okamoto, A., Higuchi, T., Hirotsu, K., Kuramitsu, S., and Kagamiyama, H. (1994) *J. Biochem. 116*, 95−107.
7. Ovchinnikov, Yu., Egorov, C. A., Aldanova, N. A., Feigina, M. Yu., Lipkin, V. M., Abdulaev, N. G., Grishin, E. V., Kiselev, A. P., Modyanov, N. N., Braunstein, A. E., Polyanovsky, O. L., and Nosikov, V. V. (1973) *FEBS Lett. 29*, 31−34.
8. Eichele, G., Karabelnik, D., Halonbrenner, R., Jansonius, J. N., and Christen, P. (1978) *J. Biol. Chem. 253*, 5239−5242.
9. Inoue, Y., Kuramitsu, S., Inoue, K., Kagamiyama, H., Hiromi, K., Tanase, S., and Morino, Y. (1989) *J. Biol. Chem. 264*, 9673−9681.
10. Kiick, D. M., and Cook, P. F. (1983) *Biochemistry 22*, 375−382.
11. Karpeisky, M. Y., and Ivanov, V. I. (1966) *Nature 210*, 493−496.
12. Ivanov, V. I., and Karpeisky, M. Y. (1969) *Adv. Enzymol. Relat. Areas Mol. Biol. 32*, 21−53.
13. Kirsch, J. F., Eichele, G., Ford, G. C., Vincent, M. G., Jansonius, J. N., Gehring, H., and Christen, P. (1984) *J. Mol. Biol. 174*, 497−525.
14. Hayashi, H., Inoue, K., Nagata, T., Kuramitsu, S., and Kagamiyama, H. (1993) *Biochemistry 32*, 12229−12239.
15. Fasella, P., Giartosio, A., and Hammes, G. G. (1966) *Biochemistry 5*, 197−202.
16. Jencks, W. P. (1969) *Catalysis in Chemistry and Enzymology*, pp 182−199, MacGraw-Hill, New York.
17. Fersht, A. L. (1985) *Enzyme Structure and Mechanism*, pp 90−91, Freeman, New York.
18. Kuramitsu, S., Hiromi, K., Hayashi, H., Morino, Y., and Kagamiyama, H. (1990) *Biochemistry 29*, 5469−5476.
19. Tonomura, B., Onishi, M., Nakatani, H., Yamaguchi-Itoh, J., and Hiromi, K. (1978) *Anal., Biochem. 84*, 370−383.
20. Kallen, R. G., Korpela, T., Martell, A. E., Matsushima, Y., Metzler, C. M., Metzler, D. E., Morozov, Yu. V., Ralston, I. M., Savin, F. A., Torchinsky, Yu., M., and Ueno, H. (1985) in *Transaminases* (Christen, P., and Metzler, D. E., Eds.) pp 37−108, John Wiley & Sons, New York.
21. Fasella, P., and Hammes, G. G. (1967) *Biochemistry 6*, 1798−1804.
22. Tobias, P. S., and Kallen, R. G. (1975) *J. Am. Chem. Soc. 97*, 6530−6539.
23. Tai, C.-H., Nalabolu, S. R., Simmons, J. W., III, Jacobson, T. M., and Cook, P. F. (1995) *Biochemistry 34*, 12311−12322.
24. Schnackerz, K. D., Tai, C.-H., Simmons, J. W., III, Jacobson, T. M., Rao, G. S. J, and Cook, P. F. (1995) *Biochemistry 34*, 12152−12160.
25. Momany, C., Ernst, S., Ghosh, R., Chang, N. L., and Hackert, M. L. (1995) *J. Mol. Biol. 252*, 643−655.
26. Hyde, C. C., Ahmed, S. A., Padlan, E. A., Miles, E. W., and Davies, D. R. (1988) *J. Biol. Chem. 263*, 17857−17871.
27. Sugio, S., Petsko, G. A., Manning, J. M., Soda, K., and Ringe, D. (1995) *Biochemistry 34*, 9661−9669.
28. Okada, K., Hirotsu, K., Sato, M., Hayashi, H., and Kagamiyama, H. (1997) *J. Biochem. 121*, 637−641.
29. Toney, M. D., Hohenester, E., Keller, J. W., and Jansonius, J. N. (1995) *J. Mol. Biol. 245*, 151−179.
30. Antson, A. A., Demidkina, T. V., Gollnick, P., Dauter, Z., von Tersch, R. L., Long, J., Berezhnoy, S. N., Phillips, R. S., Harutyunyan, E. H., and Wilson, K. S. (1993) *Biochemistry 32*, 4195−4206.
31. Sundraraju, B., Antson, A. A., Phillips, R. S., Demidkina, T. V., Barbolina, M. V., Gollnick, P., Dodson, G. G., and Wilson, K. S. (1997) *Biochemistry 36*, 6502−6510.

BI971638Z